# Detection and identification of various carbon-centred free radicals using *N*-arylketonitrones: a spin trapping/EPR/MS study

**Inas El Hassan, Laurence Charles,* Robert Lauricella and Béatrice Tuccio***

***Received (in Durham, UK) 11th September 2007, Accepted 5th December 2007***
***First published as an Advance Article on the web 20th December 2007***
**DOI: 10.1039/b713790g**

Three *N*-aryl-*C*,*C*-dimethoxycarbonylnitrones were shown to be efficient tools to detect and identify carbon-centred free radicals by coupling the spin trapping method with both EPR detection and MS/MS structure elucidation. The fragmentation pathway of these ketonitrones was first studied by MS/MS. Then, these compounds were used to trap a series of four carbon-centred free radicals and the so-formed spin adducts were analysed by the means of two techniques. EPR spectroscopy allowed to easily detect their presence in the medium, while their structure elucidation was performed using tandem mass spectrometry. The *tert*-butyl radical spin adducts showed very weak EPR signals and could not be detected by MS, probably because of a sensitivity issue. In the other cases, collision-induced dissociation of the various spin adducts mainly proceeds *via* three pathways, consisting of the elimination of the arylnitroso fragment, the radical initially trapped, or the methoxycarbonyl radical. The relative rate of these dissociations was observed to highly depend on the nature of the radical trapped. MS/MS analysis of the spin adducts allows unambiguous identification of the addends. This study also showed an unexpected reactivity of these ketonitrones towards $^{\bullet}CH_3$, resulting in the formation of EPR-silent methoxyamines. All these results demonstrate the potential of *N*-arylketonitrones in the identification of short-lived free radicals by the means of the spin trapping/EPR/MS technique.



## Introduction

Spin trapping in conjunction with electron paramagnetic resonance (EPR) spectroscopy is an efficient technique to detect free radicals produced in both chemical and biochemical processes. Ideally, it involves a reaction between a transient free radical and a diamagnetic spin trap, usually a nitrone or a nitroso compound, yielding a persistent aminoxyl radical whose EPR parameters provide information about the addend (Scheme 1).[1] Ketonitrones have been commonly used as precursors in the synthesis of natural products,[2,3] but rarely as spin traps,[4,5] while different aldonitrones have been employed in hundreds of EPR/spin trapping studies. This is partly due to the difficulty encountered in their synthesis, most of the methods commonly used to obtain aldonitrones being not transposable to the preparation of ketonitrones.[6] Another limitation to the use of ketonitrone spin traps results from the difficulty in the addend identification on the basis of the spin adduct EPR spectrum, because of the absence of hyperfine coupling with a β-hydrogen nucleus.[1,5] Note however that this lack of hydrogen in the β-position towards the nitrogen could also be an advantage since it precludes a disproportionation reaction of the aminoxyl spin adduct, thereby enhancing its life-time.

Recently, we described the synthesis of seven *N*-arylketonitrones.[7] Among them, three *N*-aryl-*C*,*C*-methoxycarbonylnitrones, namely the dimethyl [oxido(phenyl)imino]malonate **1**, the dimethyl [oxido(phenyl)imino]malonate-$d_5$ **2** and the dimethyl {[4-(methoxycarbonyl)phenyl](oxido)imino}malonate **3**, showed the most interesting performances in spin trapping chemistry (see Scheme 1). Compound **1** is very easily obtained from nitrosobenzene: its low cost synthesis allows its use in large amounts generally necessary for biological applications. Its deuterated analogue **2** yields various spin adducts with simple three line EPR signals. The particular properties of **3** results from the presence of an electron withdrawing group in the *para* position: it seems to favour the spin trapping reaction and precludes an eventual duplication of the *N*-arylaminoxyl radical.[8] These three ketonitrones were found to trap very efficiently carbon-centred free radicals in aqueous media, yielding stable aminoxyl radicals whose EPR spectra lasted several days. However, EPR signals of their various spin adducts were not very characteristic of the radical trapped. From these considerations arose the idea to combine another

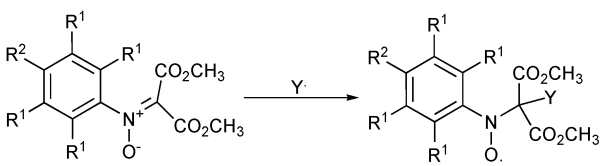


ketonitrones
**1**: $R^1 = R^2 = H$
**2**: $R^1 = R^2 = D$
**3**: $R^1 = H$, $R^2 = CO_2CH_3$

aminoxyl spin adducts
**1-Y**: $R^1 = R^2 = H$
**2-Y**: $R^1 = R^2 = D$
**3-Y**: $R^1 = H$, $R^2 = CO_2CH_3$

**Scheme 1** Spin trapping of a free radical $Y^{\bullet}$ by the ketonitrones **1–3**.

*Laboratoire TRACES, case 512, Aix-Marseille Université Faculté St Jérôme, 13397 Marseille cedex 20, France. E-mail: tuccio@up.univ-mrs.fr; laurence.charles@up.univ-mrs.fr; Fax: 33 491 282 897; Tel: 33 491 288 743*

 

analytical technique with EPR/spin trapping in order to obtain additional information on the structure of the addend.

In a previous paper, we described the application of spin trapping coupled with mass spectrometry for free radical detection using a cyclic aldonitrone, diethyl(2-methyl-1-oxido-3,4-dihydro-2*H*-pyrrol-2-yl)phosphonate (DEPMPO).[9] We thus demonstrated the feasibility of using tandem mass spectrometry for direct identification of aminoxyl spin adducts electrosprayed from complex mixture, without prior chromatographic separation. We describe herein an extension of this technique to the spin traps **1–3**. The fragmentation pathway of these *N*-arylketonitrones was first studied by tandem mass spectrometry. These compounds were then used to trap a series of carbon-centred free radicals. The corresponding spin adducts were detected by EPR spectroscopy and attempts to elucidate their structure were performed by the mean of MS/MS analysis

## Results

### Fragmentation pathway of the ketonitrones 1–3

The first synthesis of **1** was described in 2003,[3] while **2** and **3** were prepared three years later,[7] and none of these ketonitrones has ever been studied by mass spectrometry. The analysis of the fragmentation pathway of **1–3** was thus an essential step preceeding the MS/MS identification of their various spin adducts.

The positive ion ES-mass spectrum of **1** shows a major peak at *m*/*z* 238, corresponding to the protonated ketonitrone $\mathbf{[1 + H]^+}$, as well as two secondary signals at *m*/*z* 260 and 276, assigned to the sodium, $\mathbf{[1 + Na]^+}$, and potassium, $\mathbf{[1 + K]^+}$, adducts, respectively. As can be seen from Fig. 1(a), the MS/MS spectrum of *m*/*z* 238 exhibits abundant fragment ions at *m*/*z* 162, 118 and 77, beside a less important ion at *m*/*z* 206. An analysis of this MS/MS spectrum led us to propose the fragmentation pathway given in Scheme 2.

The two other *N*-aryl-*C*,*C*-dimethoxycarbonylnitrones studied, *i.e.* **2** and **3**, behaved exactly the same way as **1** in positive ion electrospray mass spectrometry. Their ESI-mass spectra exhibit a major signal attributed to the protonated ketonitrones ($\mathbf{[2 + H]^+}$ at *m*/*z* 243, $\mathbf{[3 + H]^+}$ at *m*/*z* 296), together with two less abundant peaks assigned in each case to sodium adducts ($\mathbf{[2 + Na]^+}$ at *m*/*z* 265, $\mathbf{[3 + Na]^+}$ at *m*/*z* 318) and potassium adducts ($\mathbf{[2 + K]^+}$ at *m*/*z* 281, $[\mathbf{3} + \mathrm{K}]^+$ at *m*/*z* 334). MS/MS spectra (Fig. 1(b) and (c)) indicate collision-induced dissociation of protonated ketonitrones **2** and **3** also proceeds as described for $\mathbf{[1 + H]^+}$ in Scheme 2. A methanol neutral loss (32 u) is followed by the elimination of a carbon dioxide molecule (44 u). The so-formed daughter ion further eliminates a second carbon dioxide molecule or, alternatively, a methylcyanoformate neutral (85 u).

### EPR spin trapping measurements

Though the capacity of **1–3** to act as spin trapping agents was previously demonstrated, the hyperfine coupling constants (hfccs) of the aminoxyl spin adducts were only determined in water and a wider series of carbon-centred free radicals was considered here. Throughout this text, the aminoxyl radical

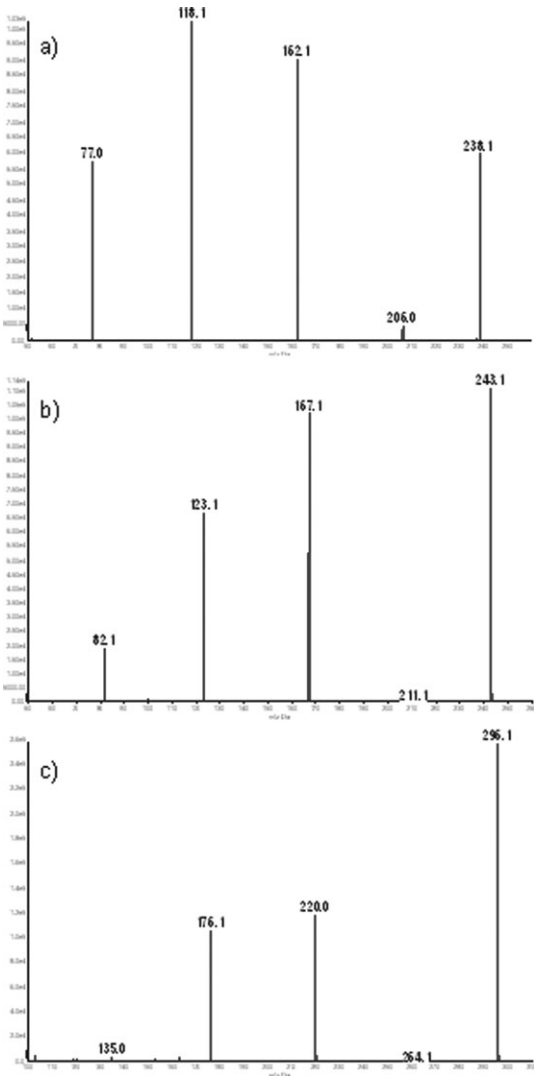


**Fig. 1** ESI-MS/MS spectra of the protonated *N*-aryl-*C*,*C*-dimethoxycarbonylnitrones (a) **1**, (b) **2** and (c) **3**.

formed by trapping a transient free radical Y$^\bullet$ by a nitrone ***n*** will be denoted ***n*-Y**, with the aim of shortening the notation (see Scheme 1). Thus, **1-$CH_2OH$** corresponds to the aminoxyl radical obtained after trapping the hydroxymethyl radical with the nitrone **1**. Four carbon-centred free radicals, *i.e.* $^\bullet CH_2OH$, $^\bullet CH(CH_3)OC_2H_5$, $^\bullet CH_3$ and $^\bullet C(CH_3)_3$, were produced in the

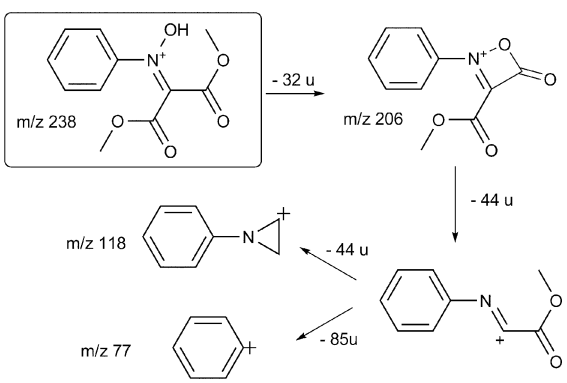


**Scheme 2** Fragmentation pattern of the protonated ketonitrone **1**.

presence of one of the three ketonitrones studied. The *ter*-butyl radical was generated by UV photolysis of the corresponding iodide, while the other free radicals were produced by reaction of $^{\bullet}OH$ on a scavenger (methanol, dimethyl sulfoxide, or diethyl ether, see Experimental section). In the case of the free radical formed after hydrogen abstraction by $^{\bullet}OH$ on diethyl ether, the question may arise whether the radical is formed on a primary or on a secondary carbon. To remove this ambiguity, an extra spin trapping experiment was performed using the 2-methyl-2-nitrosopropane (MNP) instead of **1–3**. When the Fenton reaction was performed in the presence of diethyl ether and MNP, a six-line EPR signal was recorded, because of hyperfine couplings with one nitrogen and one β-hydrogen nuclei ($a_N$ = 1.54 mT, $a_H$ = 0.21 mT). This signal can thus be assigned to the nitroxide **4**, since the nitroxide formed after trapping a radical centred on a primary carbon would have shown hyperfine coupling with two equivalent hydrogen nuclei. Consequently, this result demonstrated that, in our experimental conditions, the radical centred on a secondary carbon, *i.e.* 1-ethoxyethyl radical, was actually formed, and further trapped by **1–3**. Note also that a previous study performed with another nitroso compound spin trap, namely the diethyl (1-methyl-1-nitrosoethyl)phosphonate (DEPNP), confirmed that $^{\bullet}OH$ reaction on $(C_2H_5)_2O$ yielded the radical $^{\bullet}CH(CH_3)OC_2H_5$.[10]

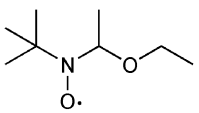


**4**

In most spin trapping experiments, an intense and very persistent EPR signal corresponding to the nitrone/free radical spin adduct considered was recorded. Note however that only weak signals were obtained when **1–3** were used to trap $^{\bullet}CH(CH_3)OC_2H_5$ and especially $^{\bullet}C(CH_3)_3$. This is likely due to steric hindrance that hampers the reaction of free radicals centred on a tertiary or a secondary carbon with ketonitrones. The general shape of the EPR spectra varies with the nitrone spin trap (see Fig. 2). Whatever the radical trapped by **1**, the EPR signal recorded consisted in three main lines, due to a hyperfine coupling with the nitrogen nucleus (hfcc: $a_N$), greatly broadened or multiplied because of hyperfine couplings with

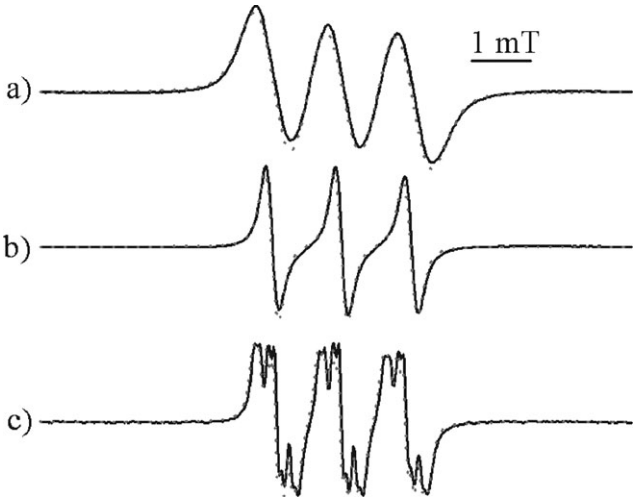


**Fig. 2** EPR spectra of (a) **1-CH$_2$OH**, (b) **2-CH$_2$OH** and (c) **3-CH$_2$OH**, recorded in water–methanol (4 : 1, v/v) after argon bubbling, and their superimposed simulations (dotted lines) which led to the parameters listed in Table 1.

aromatic hydrogen nuclei (hfcc: $a_{Harom}$). The presence of a substituting group in the *para* position in **3** allowed a narrower spectra to be obtained by reducing the number of aromatic hydrogen nuclei. Using the spin trap **2** instead of **1** or **3** led to aminoxyl spin adducts showing much simpler EPR spectra, consisting of three lines only. To illustrate this, the EPR signals of **1-CH$_2$OH**, **2-CH$_2$OH** and **3-CH$_2$OH** have been reproduced in Fig. 2, along with their superimposed simulation. The hfccs listed in Table 1 have been evaluated for the various spin adducts by simulating all the spectra recorded. As noticed earlier,[7] $a_N$ determined for each spin adduct was found very sensitive to the solvent polarity. In the case of **1-CH$_2$OH** for instance, $a_N$ varies from 1.20 mT in water to 1.10 mT in $CH_2Cl_2$.[7] However, the hfccs listed in Table 1 are not characteristic of the radical trapped. Whatever the nitrone, the different spin adducts of carbon-centred free radicals exhibited almost identical spectra. This underlines the limitation of the EPR/spin trapping technique, more particularly when ketonitrone spin traps are employed: it does not allow unambiguous identification of the radical initially trapped. Nevertheless, the

**Table 1** EPR hyperfine coupling constants $a_N$ and $a_{Harom}$, for various spin adducts of the *N*-aryl-*C*,*C*-dimethoxycarbonylnitrones **1–3**

| Spin adduct | $a_N$/mT | $a_{Harom}$/mT | Solvent |
|---|---|---|---|
| **1-CH$_2$OH** | 1.17 | 0.12 (2H); 0.25 (3H) | Water–methanol[a] |
| **1-CH(CH$_3$)OC$_2$H$_5$** | 1.10 | 0.19 (2H); 0.21 (3H) | Water–benzene–Et$_2$O[b] |
| **1-CH$_3$** | 1.24 | 0.10 (2H); 0.22 (3H) | Water–DMSO[a] |
| **1-C(CH$_3$)$_3$** | 1.04 | 0.11 (2H); 0.23 (3H) | Benzene |
| **2-CH$_2$OH** | 1.17 | — | Water–methanol[a] |
| **2-CH(CH$_3$)OC$_2$H$_5$** | 1.11 | — | Water–benzene–Et$_2$O[b] |
| **2-CH$_3$** | 1.23 | — | Water–DMSO[a] |
| **2-C(CH$_3$)$_3$** | 1.05 | — | Benzene |
| **3-CH$_2$OH** | 1.10 | 0.09 (2H); 0.24 (2H) | Water–methanol[a] |
| **3-CH(CH$_3$)OC$_2$H$_5$** | 1.04 | 0.09 (2H); 0.22 (2H) | Water–benzene–Et$_2$O[b] |
| **3-CH$_3$** | 1.13 | 0.09 (2H); 0.24 (2H) | Water–DMSO[a] |
| **3-C(CH$_3$)$_3$** | 0.99 | 0.05 (2H); 0.24 (2H) | Benzene |

[a] 4 : 1, v/v. [b] 4 : 1 : 1, v/v/v.

 

crucial role of this preliminary EPR analysis was to demonstrate the presence of paramagnetic spin adducts in the medium before MS experiments.

### ESI-MS and MS/MS analysis of the spin adducts

All the spin trapping experiments were first performed as indicated in the Experimental section. Then, the samples were evaporated under reduced pressure to remove the solvent, eventually after extraction with $CH_2Cl_2$ when the spin adduct was primarily formed in aqueous media, before being dissolved in acidified methanol for MS analysis. Using this spin trapping/MS approach, we never succeeded to detect the free radical $^{\bullet}C(CH_3)_3$. After trapping this radical with **1–3**, the spin adducts obtained gave only weak EPR signals despite the high sensitivity of this spectroscopy, suggesting their concentration is below the MS detection limit. In all the other cases, the results obtained are described hereafter.

When this technique was applied to **1-$CH_2OH$**, the positive ion ES mass spectrum showed the presence of a peak at *m*/*z* 269, assigned to **[1-$CH_2OH$ + H]$^+$** on the basis of accurate mass measurements ($C_{12}H_{15}NO_6^{+\cdot}$, *m*/*z* 269.0893, double bond equivalents, DBE = 6). MS/MS data (Fig. 3(a)) were shown to be consistent with the expected ion structures. By far, the most abundant fragment ion was detected at *m*/*z* 162. It arose from the loss of nitrosobenzene ($C_6H_5 - NO$) in a very fast reaction, which is consistent with a radical-initiated rupture. The structure of the so-obtained fragment ion, $[^{\bullet}C(CH_2OH)(CO_2CH_3)_2 + H]^+$, was confirmed by accurate mass measurements ($C_6H_{10}O_5^{+}$, *m*/*z* 162.0522, DBE = 2). This stable radical cation further decomposed to yield low intensity peaks at *m*/*z* 145 and 144, corresponding to the loss of $^{\bullet}OH$ and $H_2O$, respectively. Beside this major fragmentation pathway, **[1-$CH_2OH$ + H]$^+$** was also found to decompose according to several other minor routes. Notably, loss of a methoxycarbonyl radical was shown to lead to *m*/*z* 210 ($C_{10}H_{12}NO_4^{+}$, *m*/*z* 210.0760, DBE = 5.5) and elimination of the hydroxymethyl radical initially trapped gave rise to *m*/*z* 238 ($C_{11}H_{12}NO_5^{+}$, *m*/*z* 238.0709, DBE = 6.5). When used to detect $^{\bullet}CH_2OH$, the two other ketonitrones gave similar results, as can be seen from Fig. 3. In each case, the fastest dissociation reaction produced the protonated radical, $[^{\bullet}C(CH_2OH)(CO_2CH_3)_2 + H]^+$, detected at *m*/*z* 162, after elimination of either nitrosobenzene-$d_5$ or methyl 4-nitrosobenzoate from **[2-$CH_2OH$ + H]$^+$** and **[3-$CH_2OH$ + H]$^+$**, respectively. To a lesser extent, the fragmentation of **[2-$CH_2OH$ + H]$^+$** and **[3-$CH_2OH$ + H]$^+$** also proceeded *via* the release of $^{\bullet}CH_2OH$ (to respectively yield *m*/*z* 243 and 296) or of $^{\bullet}C(O)OCH_3$ (to give rise to *m*/*z* 215 and 268, respectively).

The spin adducts formed by trapping the free radical derived from $C_2H_5OC_2H_5$ by the nitrones **1–3** were also analysed in positive mode electrospray mass spectrometry. As in the case of the spin adducts ***n*-$CH_2OH$**, the three ketonitrones behaved the same, showing that the nature of the aryl group had no influence on the decomposition process of the spin adducts ***n*-$CH(CH_3)OC_2H_5$**. In order to avoid useless repetitions, only the case of **1-$CH(CH_3)OC_2H_5$** will be fully described. After the spin trapping reaction, MS

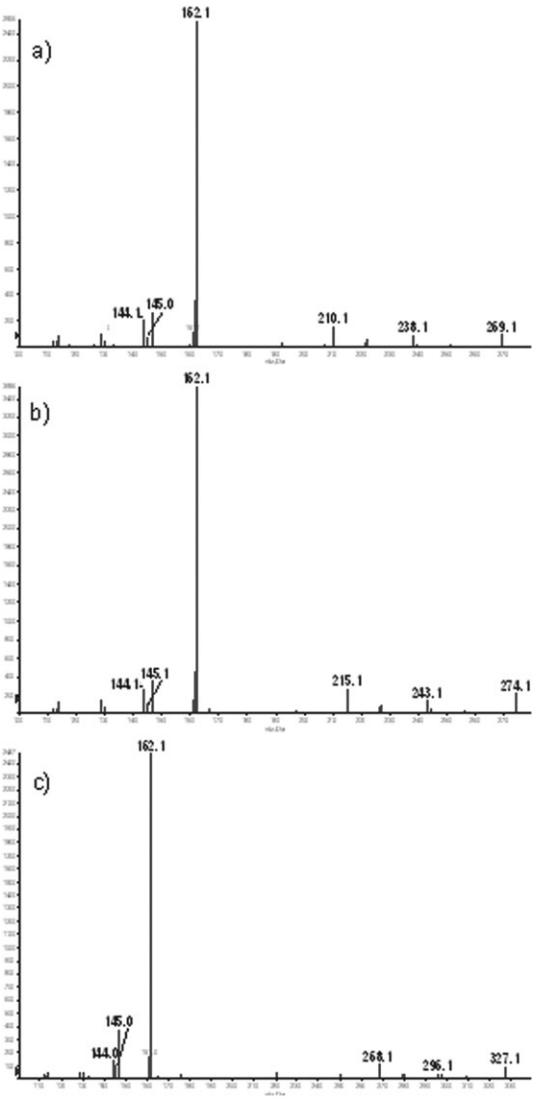


**Fig. 3** ESI-MS/MS spectra of (a) **[1-$CH_2OH$ + H]$^+$**, (b) **[2-$CH_2OH$ + H]$^+$** and (c) **[3-$CH_2OH$ + H]$^+$**.

analysis revealed the presence of a peak at *m*/*z* 311 assigned to **[1-$CH(CH_3)OC_2H_5$ + H]$^+$** on the basis of its accurate mass measurement ($C_{15}H_{21}NO_6^{+\bullet}$, *m*/*z* 311.1363, DBE = 6). ESI-MS/MS spectrum of this radical cation is described in Table 2.

The most abundant fragment ion was observed at *m*/*z* 238. It would correspond to the loss of the radical initially trapped, releasing the protonated ketonitrone **[1 + H]$^+$** (*m*/*z* 238) which further decomposed to yield *m*/*z* 162. Beside this major

**Table 2** Peaks observed in the ESI-MS/MS spectrum of the protonated spin adduct **[1-$CH(CH_3)OC_2H_5$ + H]$^+$** (*m*/*z* 311)

| Ion *m*/*z* | Relative intensity (%) | Formula | DBE |
|---|---|---|---|
| 311.1363 | 35.8 | $C_{15}H_{21}NO_6^{+\bullet}$ | 6 |
| 279.1101 | 4.2 | $C_{14}H_{17}NO_5^{+\bullet}$ | 7 |
| 239.0788 | 30.8 | $C_{11}H_{13}NO_5^{+\bullet}$ | 6 |
| 238.0709 | 100 | $C_{11}H_{12}NO_5^{+}$ | 6.5 |
| 223.0839 | 3.3 | $C_{11}H_{13}NO_4^{+\bullet}$ | 6 |
| 222.0760 | 44.2 | $C_{11}H_{12}NO_4^{+}$ | 6.5 |
| 221.0682 | 26.7 | $C_{11}H_{11}NO_4^{+\bullet}$ | 7 |
| 162.0549 | 5.0 | $C_9H_8NO_2^{+}$ | 6.5 |

process, other pathways involving various molecular rearrangements, leading to the loss of methanol (−32 u), ethoxyethylene (−72 u), ethyl acetate (−88 u), ethoxy(methoxy)methyl radical (−89 u) and (methoxymethoxy)ethane (−90 u), were also found to contribute to the fragmentation pattern of **[1-CH(CH$_3$)OC$_2$H$_5$ + H]$^+$** (Scheme 3). It is worth mentioning that, in contrast to the spin adducts obtained after trapping the hydroxymethyl radical, **[1-CH(CH$_3$)OC$_2$H$_5$ + H]$^+$** never decomposed *via* the release of the nitrosobenzene. Analogous results were obtained with **2-CH(CH$_3$)OC$_2$H$_5$** and **3-CH(CH$_3$)OC$_2$H$_5$**, with a major fragmentation pathway corresponding to the release of the radical •CH(CH$_3$)OC$_2$H$_5$.

Mass spectrometric study of spin adducts obtained after trapping the methyl radical by **1–3** revealed a particular reactivity of these ketonitrones towards •CH$_3$. In the positive mode ESI mass spectrum of the mixture obtained after generating the methyl radical in the presence of **1**, only a very weak peak is observed for the expected **[1-CH$_3$ + H]$^+$** at *m*/*z* 253 whereas an intense signal is measured at *m*/*z* 268. The latter peak could be assigned to the protonated methoxyamine **5**, potentially formed after double spin trapping of the methyl radical by the ketonitrone **1** (see Scheme 4). In order to confirm these assignments, both ions were submitted to fragmentation for structural elucidation. Due to the low abundance of the precursor ion, signals observed in the MS/MS spectrum of *m*/*z* 253 were of weak intensity. Nevertheless, a major fragment ion could be measured at *m*/*z* 146 and would indicate the loss of a nitrosobenzene molecule from the precursor ion. A less favoured process, yielding a peak at *m*/*z* 194, would consist of the elimination of a methoxycarbonyl radical (59 u) from **[1-CH$_3$ + H]$^+$**. MS/MS data obtained from *m*/*z* 268 are described in Table 3 and would be consistent with the fragmentation pattern of **[5 + H]$^+$** as proposed in Scheme 5(a).

The same experiments were performed with the nitrone **2** and similar results were obtained. A weak signal was obtained at *m*/*z* 258 for **[2-CH$_3$ + H]$^+$** while a more intense peak,

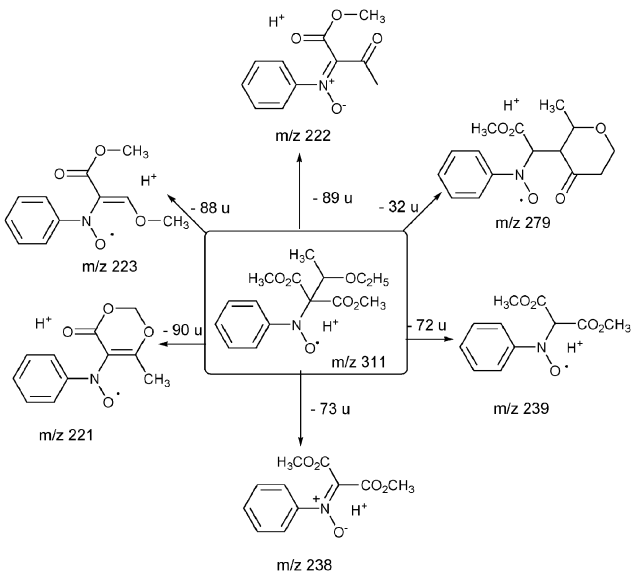


**Scheme 3** Fragmentation pattern of the protonated spin adduct **[1-CH(CH$_3$)OC$_2$H$_5$ + H]$^+$**.

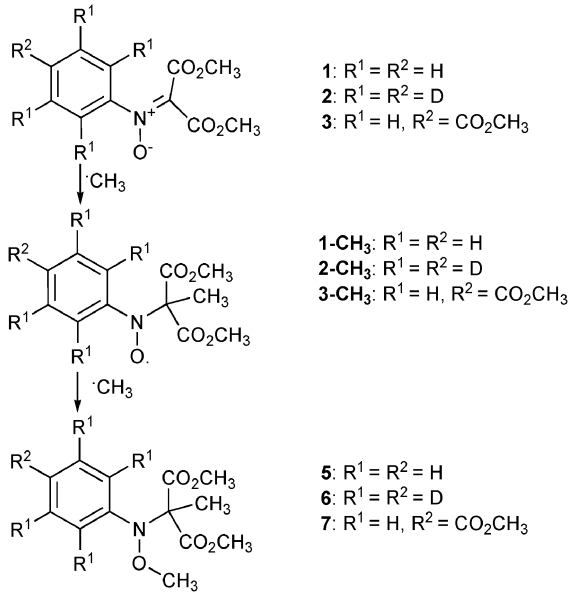


**Scheme 4** Formation of the methoxyamines **5–7** after double spin trapping of the methyl radical by the ketonitrones **1–3**.

observed at *m*/*z* 273, was assigned to the protonated methoxyamine **6**. No MS/MS data could be obtained for the low abundance **[2-CH$_3$ + H]$^+$**. In contrast, collision-induced dissociation of **[6 + H]$^+$** yielded daughter ions with a 5 u mass shift as compared to fragments arising from **[5 + H]$^+$**, indicating similar fragmentation pathways as proposed in Scheme 5(a). However, in addition to the expected *m*/*z* 137 ion, a more intense peak was observed at *m*/*z* 136 in the MS/MS spectrum of **[6 + H]$^+$**. This indicates the mechanism proposed for the formation of *m*/*z* 132 in Scheme 5(a) would be a low rate reaction and that an alternative fragmentation process, involving the elimination of a neutral containing an aromatic proton, should be envisaged.

The mechanism proposed in Scheme 5(b) would account for the ion filiation *m*/*z* 273 → *m*/*z* 241 → *m*/*z* 197 → *m*/*z* 136 in the **[6 + H]$^+$** MS/MS spectrum. Indeed, the deuterium atom, initially in *ortho* position on the aromatic ring and then transferred onto the nitrogen atom in *m*/*z* 197, would be contained in the neutral, *i.e.*, DC(O)OCH$_3$ (61 u), consecutively lost to produce *m*/*z* 136.

When the methyl radical was produced in the presence of **3** as indicated in the Experimental section, the ESI-MS spectrum of the mixture exhibited peaks at *m*/*z* 311 and 326, respectively

**Table 3** Peaks observed in the ESI-MS/MS spectrum of the protonated methoxyamine **5** (*m*/*z* 268)

| Ion *m*/*z* | Relative intensity (%) | Formula | DBE |
|---|---|---|---|
| 268.1179 | 100 | $C_{13}H_{18}NO_5^+$ | 5.5 |
| 237.0996 | 21.2 | $C_{12}H_{15}NO_4^{+\bullet}$ | 6 |
| 236.0917 | 50.0 | $C_{12}H_{14}NO_4^+$ | 6.5 |
| 204.0655 | 33.3 | $C_{11}H_{10}NO_3^+$ | 7.5 |
| 192.1019 | 37.9 | $C_{11}H_{14}NO_2^+$ | 5.5 |
| 178.0863 | 10.7 | $C_{10}H_{12}NO_2^+$ | 5.5 |
| 176.0706 | 13.6 | $C_{10}H_{10}NO_2^+$ | 6.5 |
| 132.0807 | 65.2 | $C_9H_{10}N^+$ | 5.5 |
| 118.0651 | 10.2 | $C_8H_8N^+$ | 5.5 |

 

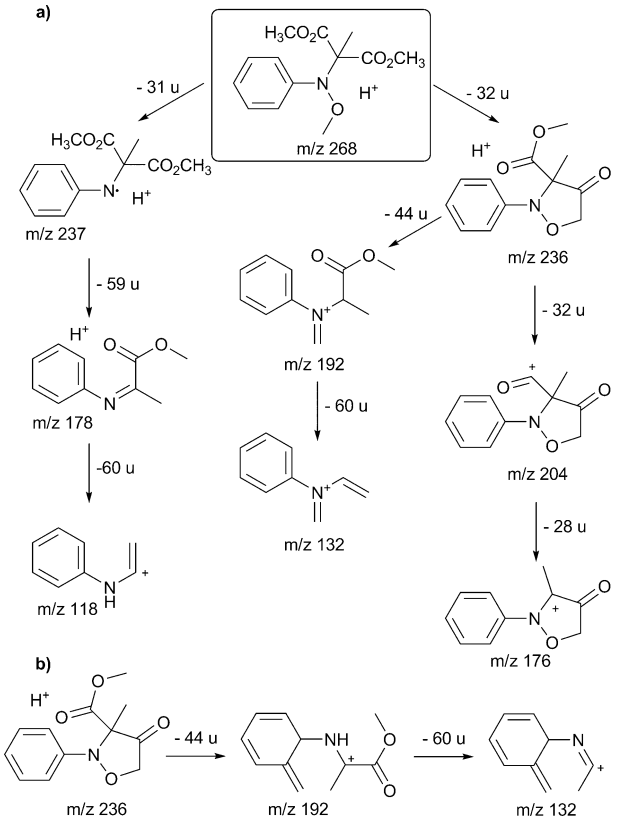


**Scheme 5** (a) Fragmentation pattern of the protonated methoxyamine **5** and (b) alternative reaction pathway to produce *m*/*z* 132 from *m*/*z* 236.

assigned to **[3-CH$_2$OH + H]$^+$** and the protonated methoxyamine **7**.

As compared to **1-CH$_3$** and **2-CH$_3$**, the signal of **[3-CH$_2$OH + H]$^+$** was much higher in the MS spectrum and could allow better quality MS/MS data to be obtained. Collision-induced dissociation of *m*/*z* 311 produced a main fragment ion at *m*/*z* 146, resulting from the loss of an arylnitroso compound, *i.e.*, *para*-$CH_3O_2C$–$C_6H_4$–NO. The so-obtained radical cation further eliminated a methanol molecule to yield *m*/*z* 114. In a much less favoured process, the precursor ion was also observed to fragment *via* the loss of a methoxycarbonyl radical, as reported from the MS/MS experiments performed with **[1-CH$_3$ + H]$^+$**. The main daughter ions arising from collision-induced dissociation of *m*/*z* 326 were detected at *m*/*z* 295, 294, 262, 250, 236, 234, 190 and 176, as expected for fragmentation of **[7 + H]$^+$** according to Scheme 5.

## Discussion

The various spin adducts ***n*-Y** considered in this study were found to be very stable in solution, their EPR signal showing no significant decrease for weeks. However, the capacity of **1–3** to act as spin trapping agents seems to be lowered by an increase in the steric hindrance of **Y**. Though the kinetic aspects of the trapping reaction using **1–3** have not been investigated, it is worth mentioning that ketonitrones are generally considered to scavenge free radicals more slowly than aldonitrones.[4,11]

Collision induced dissociation of the various spin adducts considered was shown to proceed *via* different pathways, depending on the structure of the trapped radical. Competing processes, which released the arylnitroso moiety, the •Y radical initially trapped or a methoxycarbonyl radical, were most frequently observed. Results obtained for each spin adduct with regard to these three reactions have been summarised in Table 4. The relative rate of reactions yielding radical moieties during collision-induced dissociations of protonated ***n*-Y** (Y = $CH_3$ or $CH_2OH$) could be related to radical relative stabilities, as expected from radical cation fragmentation rules.[12] The major loss of arylnitroso neutrals from **[*n*-CH$_3$ + H]$^+$** could actually be considered as a very favored formation of $^\bullet C(CH_3)(CO_2CH_3)_2$, detected as a protonated radical at *m*/*z* 162 in MS/MS. The heat of formation was found to be much higher for this radical (−607.6 kJ mol$^{-1}$)[13,14] than for methoxycarbonyl radical (−169.6 kJ mol$^{-1}$).[14] Accordingly, the absence of methyl radical loss would be consistent with the low stability of this radical ($\Delta H^\circ_f(^\bullet CH_3)$ = +145.7 kJ mol$^{-1}$).[15] Similarly, MS/MS results observed for protonated spin adducts obtained after trapping $^\bullet CH_2OH$ radical with **1–3** could also be accounted for by comparing radicals in terms of heat of formation in the gas phase: $^\bullet CH_2OH$ (−9 kJ mol$^{-1}$)[16] < $^\bullet C(O)OCH_3$ (−170 kJ mol$^{-1}$) < $^\bullet C(CH_2OH)(CO_2CH_3)_2$ (−802 kJ mol$^{-1}$). These results are consistent with data obtained for carbon-centred radical spin adducts of DEPMPO.[9] In contrast, the unique MS/MS

**Table 4** Main competing fragmentation processes observed during the collision induced dissociation of the protonated aminoxyl spin adduct ***n*-Y** formed after the trapping of a free radical Y• by the ketonitrones **1–3**

| Y• | n | Precursor ion | Major loss | Competing fragmentation processes (minor loss) | Comments |
|---|---|---|---|---|---|
| $^\bullet CH_3$ | 1 | **[1-CH$_3$ + H]$^+$** | Ar-NO[a] | $^\bullet CO_2CH_3$ | No loss of Y• |
| | 2 | **[2-CH$_3$ + H]$^+$** | * | * | |
| | 3 | **[3-CH$_3$ + H]$^+$** | Ar-NO[c] | $^\bullet CO_2CH_3$ | No loss of Y• |
| $^\bullet CH_2OH$ | 1 | **[1-CH$_2$OH + H]$^+$** | Ar-NO[a] | Y• and $^\bullet CO_2CH_3$ | |
| | 2 | **[2-CH$_2$OH + H]$^+$** | Ar-NO[b] | Y• and $^\bullet CO_2CH_3$ | |
| | 3 | **[3-CH$_2$OH + H]$^+$** | Ar-NO[c] | Y• and $^\bullet CO_2CH_3$ | |
| $^\bullet CH(CH_3)OC_2H_5$ | 1 | **[1-CH(CH$_3$)OC$_2$H$_5$ + H]$^+$** | Y• | Various neutral losses after molecule rearrangement | No loss of Ar-NO[a] or $^\bullet CO_2CH_3$ |
| | 2 | **[2-CH(CH$_3$)OC$_2$H$_5$ + H]$^+$** | Y• | Various neutral losses after molecule rearrangement | No loss of Ar-NO[a] or $^\bullet CO_2CH_3$ |
| | 3 | **[3-CH(CH$_3$)OC$_2$H$_5$ + H]$^+$** | Y• | Various neutral losses after molecule rearrangement | No loss of Ar-NO[a] or $^\bullet CO_2CH_3$ |

[a] Ar- = $C_6H_5$. [b] Ar- = $C_6D_5$. [c] Ar- = *para*-$CH_3O_2CC_6H_4$–; * no MS/MS data available due to precursor ion very low abundance.

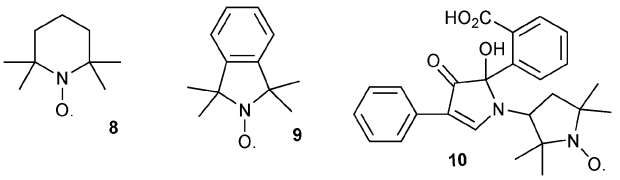


**Scheme 6** Examples of stable aminoxyl radicals used as spin traps.

reaction producing a radical moiety from $\mathbf{[\textit{n}\text{-}CH(CH_3)OC_2H_5 + H]^+}$ consists of the loss of the radical initially trapped, *i.e.*, $^{\bullet}CH(CH_3)OC_2H_5$, which heat of formation was found to be $-81.2$ kJ mol$^{-1}$.[14] This result is unexpected in terms of relative radical stability: elimination of a methoxycarbonyl radical ($-170$ kJ mol$^{-1}$) or formation of the radical ($-820$ kJ mol$^{-1}$) associated to the elimination of arylnitroso neutral would have been more favoured but were not observed. Alternatively, the particular MS/MS behaviour of $\mathbf{[\textit{n}\text{-}CH(CH_3)OC_2H_5 + H]^+}$ might be accounted for by considering the higher steric hindrance of $-CH(CH_3)OC_2H_5$ as compared to a methyl or a hydroxymethyl group.

When the methyl radical was produced in the presence of one of the ketonitrones studied, protonated spin adduct $\mathbf{\textit{n}\text{-}CH_3}$ were hardly observed in positive mode ESI-MS, whereas all the three aminoxyl spin adducts $\mathbf{1\text{-}CH_3}$, $\mathbf{2\text{-}CH_3}$ and $\mathbf{3\text{-}CH_3}$ were detected by EPR spectroscopy. However, in each case, MS analysis showed the presence of an EPR-silent methoxyamine, likely formed after double spin trapping of the methyl radical (see Scheme 4). Some stable aminoxyl radicals can be used as spin trapping agents to remove free radicals. In this method, known as the "aminoxyl (or nitroxide) trapping technique", a coupling reaction occurs between the aminoxyl and the alkyl free radical, thereby yielding an alkoxyamine.[17] Examples of stable aminoxyl traps used in this method are shown in Scheme 6. In general, they possess quaternary carbons in the two α-position towards the aminoxyl nitrogen (*e.g.* **8–10**). To our knowledge, no *N*-aryl aminoxyl have ever been used to scavenge free radicals. The spin density on the aminoxyl oxygen is lowered by conjugation with the aryl moiety, thereby rendering these molecules less prone to radical coupling. MS analysis has demonstrated the capacity of the stable aminoxyls $\mathbf{1\text{-}CH_3}$, $\mathbf{2\text{-}CH_3}$ and $\mathbf{3\text{-}CH_3}$ to trap the methyl radical leading to the corresponding methoxyamines **5–7**. Note however that no other alkoxyamine has ever been detected by mass spectrometry in our experiments, showing that the aminoxyl spin adducts $\mathbf{\textit{n}\text{-}Y}$ were unable to scavenge the other free radicals $Y^{\bullet}$ considered in this study. This could be related to the free radical relative stabilities, the methyl radical being the most reactive in the series studied. Note also that the presence of the *para*-methoxycarbonyl group in the ketonitrone **3** diminishes the reactivity of $\mathbf{3\text{-}CH_3}$ towards $^{\bullet}CH_3$, which would explain the higher abundance of protonated aminoxyl $\mathbf{3\text{-}CH_3}$, as compared to $\mathbf{1\text{-}CH_3}$ and $\mathbf{2\text{-}CH_3}$, in mass spectrometry.

## Experimental

### Materials

The nitrones **1–3** were synthesised, purified and identified in our laboratory after procedures extensively described previously.[7] All chemicals, including the 2-methyl-2-nitrosopropane (MNP), were purchased from Sigma-Aldrich (St. Louis, MO) and used without further purification. The solvents were of the highest purity commercially available and used as received. Aqueous media were prepared from tridistilled water.

### Spin trapping experiments

Spin trapping experiments were performed in water or benzene, by using two different procedures to generate the various carbon-centred free radicals in the presence of each of the ketonitrones. The radicals $^{\bullet}CH_3$, $^{\bullet}CH_2OH$ and $^{\bullet}CH(CH_3)OC_2H_5$ were produced in water in the presence of **1**, **2** or **3** (20 mmol dm$^{-3}$) by performing a standard Fenton reaction (0.4% $H_2O_2$, 10 mmol dm$^{-3}$ $FeSO_4$) in the presence dimethyl sulfoxide (DMSO, 20%), methanol (20%), or diethyl ether (20%), respectively. The systems were allowed to react for 1–2 min, and the medium was briefly extracted with dichloromethane. The radical $^{\bullet}C(CH_3)_3$ was generated by UV-photolysis of a benzene solution of *ter*-butyl iodide (1.5 mol dm$^{-3}$). Whatever the generating system, an aliquot (*ca.* 50 mm$^3$) of the organic phase was analysed by EPR spectroscopy after argon bubbling, while the remaining sample was evaporated under reduced pressure to remove the solvent before being dissolved in acidified methanol for MS analysis.

In the case of the radical derived from diethyl ether, a spin trapping reaction followed by EPR detection was also performed using the nitroso spin trap MNP. The carbon-centred free radical was produced in the presence of MNP (30 mmol dm$^{-3}$) by conducting a Fenton reaction in water–benzene–diethyl ether (4 : 1 : 1, v/v/v).

### CW-EPR detection

EPR assays were performed at room temperature in capillary tubes. EPR spectra were recorded on a continuous-wave (CW) spectrometer Bruker EMX operating at X-band. The following conditions were used: modulation frequency, 100 kHz; non-saturating microwave power, 20 mW; modulation amplitude, from 0.05 to 0.1 mT; receiver gain, from $5 \times 10^5$ to $10^6$; time constant, 82 to 164 ms; scan time, from 42 to 84 s; scan width, from 4 to 6 mT; 1 scan. All the EPR spectra recorded were analysed by simulation using the software elaborating by Duling, which permits to fit a calculated spectrum to an experimental one.[18]

### Mass spectrometry

All experiments were performed with a QStar Elite mass spectrometer (Applied Biosystems SCIEX, Concord, ON, Canada) equipped with an electrospray ionization source operated in the positive ion mode. The capillary voltage was set at 5500 V and the cone voltage at 60 V. In this hybrid instrument, ions were measured using an orthogonal acceleration time-of-flight (oa-TOF) mass analyzer. A quadrupole was used for selection of precursor ions to be further submitted to collision-induced dissociation (CID) in MS/MS experiments. Nitrogen was used as the nebulizing gas (20 psi), the curtain gas (20 psi) as well as the collision gas. Collision energies were in the range 10–15 eV (laboratory frame). Accurate mass



 

measurements, performed using internal calibration, allowed elemental composition and the number of double bond equivalents (DBEs) to be reached for each targeted ion. DBE corresponds to the number of double bonds and rings. In case of an even-electron state ion, add 0.5 to convert the reported DBE value to the actual number of double bonds.[12] Analyst software version 2.1 was used for instrument control, data acquisition and data processing. Direct sample introduction was performed at a 5 μL $min^{-1}$ flow rate using a syringe pump.

### Heats of formation

Heats of formation in the gas phase of some radicals could not be found in the literature. A low performance calculation (CS MOPAC, AM1) was thus performed. The following values were obtained: $\Delta H^\circ_f(^\bullet CH_3) = +130.6$ kJ $mol^{-1}$, $\Delta H^\circ_f(^\bullet CH_2OH) = -111.0$ kJ $mol^{-1}$, $\Delta H^\circ_f[^\bullet CH(CH_3)OC_2H_5] = -158.8$ kJ $mol^{-1}$, $\Delta H^\circ_f[^\bullet C(O)OCH_3] = -210.0$ kJ $mol^{-1}$, $\Delta H^\circ_f[^\bullet C(CH_3)(CO_2CH_3)_2] = -616.0$ kJ $mol^{-1}$, $\Delta H^\circ_f[^\bullet C(CH_2OH)(CO_2CH_3)_2] = -801.7$ kJ $mol^{-1}$, and $\Delta H^\circ_f\{^\bullet C[CH(CH_3)OC_2H_5](CO_2CH_3)_2\} = -820.0$ kJ $mol^{-1}$. Comparison with referenced data indicates the absolute calculated values are very approximate ($\Delta H^\circ_f(^\bullet CH_3) = +145.7$ kJ $mol^{-1}$,[15] $\Delta H^\circ_f(^\bullet CH_2OH) = -9.0$ kJ $mol^{-1}$,[16] $\Delta H^\circ_f[^\bullet CH(CH_3)OC_2H_5] = -81.2$ kJ $mol^{-1}$,[14] $\Delta H^\circ_f[^\bullet C(O)OCH_3] = -169.6$ kJ $mol^{-1}$,[12] $\Delta H^\circ_f[^\bullet C(CH_3)(CO_2CH_3)_2] = -607.6$ kJ $mol^{-1}$,[13,14]) but could be used to validate the relative stability scale.

## Conclusions

This study clearly confirm the relevance of tandem mass spectrometry for direct identification of free radical spin adducts from complex mixture, without preliminary chromatographic separation. In this field, *N*-aryl-*C*,*C*-dialkoxycarbonylnitrones such as **1–3** could find interesting applications in both radical chemistry and biochemistry.

First, the versatility of their synthesis pathway would permit to prepare a much wider range of nitrones in this series, bearing different functional groups and showing various properties.[7] For example, it could be possible to prepare *N*-arylketonitrones that could be covalently linked to natural or synthetic macromolecules, or able to cross biological membranes and enter the cells. In addition, the spin adducts obtained after trapping free radicals by ketonitrones do not disproportionate, which enhances their lifetime. Thus, the various carbon-centred radical spin adducts ***n*-Y** considered in this study were found to be stable for weeks in organic media. Note however that, generally speaking, the efficiency of spin trapping reactions is altered by the presence of bulky groups born on either the nitronyl-carbon or the free radical centre. These considerations let us think that *N*-arylketonitrones could be very efficient tools for qualitative studies, but their use for free radical quantification should be avoided.

Though EPR signals of **1–3** various spin adducts were not characteristic of the radical trapped, EPR analysis permitted to prove the presence of paramagnetic species in the medium. Collision-induced dissociation of the various spin adducts mainly proceeds *via* three pathways, consisting of the elimination of the arylnitroso fragment, the radical initially trapped, or the methoxycarbonyl radical. The relative rate of these dissociations was observed to highly depend on the nature of the radical trapped. MS/MS analysis of the spin adduct allows unambiguous identification of the addend. This study also showed an unexpected reactivity of these ketonitrones towards $^\bullet CH_3$, resulting in the formation of EPR-silent methoxyamines. The feasibility of this approach should generate a renewal of interest for ketonitrone spin traps, since the results presented herein demonstrate the potential of *N*-arylketonitrones in the identification of short-lived free radicals.

## Acknowledgements

L. C. acknowledges support from Spectropole, the Analytical Facility of Aix-Marseille University, by allowing a special access to the instruments purchased with European Funding (FEDER OBJ2142-3341).

## References

1 (*a*) E. Janzen, *Acc. Chem. Res.*, 1971, **4**, 31; (*b*) A. Evans, *Aldrichimica Acta*, 1979, **12**, 23; (*c*) R. Buettner, *Free Radical Biol. Med.*, 1987, **3**, 549, and references therein; (*d*) P. Tordo, *Electron Paramagn. Reson.*, 1998, **16**, 116, and references therein.
2 (*a*) C. W. Holzapfeland and R. Crous, *Heterocycles*, 1988, **48**, 1337; (*b*) S. Torrente, B. Noya, V. Brandchadell and R. Alonso, *J. Org. Chem.*, 2003, **68**, 4772; (*c*) R. Fischer, E. Hyrgova, L. Fisera, C. Hametner and M. Cyranski, *Chem. Pap.*, 2005, **59**, 275.
3 Y. Tomioka, C. Nagahiro, Y. Nomura and H. Maruoka, *J. Heterocycl. Chem.*, 2003, **40**, 121.
4 E. Finkelstein, G. M. Rosen, E. J. Rauckman and J. Paxton, *Mol. Pharmacol.*, 1979, **16**, 676.
5 (*a*) M. Nishi, A. Hagi, H. Ide, A. Murakami and K. Makino, *Biochem. Int.*, 1992, **27**, 651; (*b*) E. G. Janzen and Y. K. Zhang, *J. Magn. Reson., Ser. B*, 1993, **101**, 91; (*c*) G. M. Rosen, P. Tsai, E. D. Barth, G. Dorey, P. Casara, M. Spedding and H. J. Halpern, *J. Org. Chem.*, 2000, **65**, 4460; (*d*) S. Bottle and A. Micallef, *Org. Biomol. Chem.*, 2003, **1**, 2581; (*e*) J. Boyer, V. Bernardes-Genisson, V. Farines, J.-P. Souchard and F. Nepveu, *Free Radical Res.*, 2004, **38**, 459; (*f*) C. Sar, E. Osz, J. Jeko, J.-P. Souchard and K. Hideg, *Synthesis*, 2005, **2**, 255; (*g*) K. Reybier, J. Boyer, V. Farines, F. Camus, J.-P. Souchard, M.-C. Monje, V. Bernardes-Genisson, S. Goldstein and F. Nepveu, *Free Radical Res.*, 2006, **40**, 11; (*h*) P. Ionita, *Free Radical Res.*, 2006, **40**, 59.
6 (*a*) K. G. B. Torsell, in *Nitrile Oxides, Nitrones and Nitronates in Organic Synthesis*, VCH Inc., New York, 1988; (*b*) S. Franco, F. L. Merchán, P. Merino and T. Tejero, *Synth. Commun.*, 1995, **25**, 2275.
7 I. El Hassan, R. Lauricella and B. Tuccio, *Cent. Eur. J. Chem.*, 2006, **4**, 338.
8 A. Calder and A. Forrester, *Chem. Commun.*, 1967, 652.
9 B. Tuccio, R. Lauricella and L. Charles, *Int. J. Mass Spectrom.*, 2006, **252**, 47.
10 V. Roubaud, C. Rizzi, S. Guérin, R. Lauricella, J. C. Bouteiller and B. Tuccio, *Free Radical Res.*, 2001, **34**, 237.
11 Y. Sueishi, D. Yoshioka, C. Yoshioka, S. Yamamoto and Y. Kotake, *Org. Biomol. Chem.*, 2006, **4**, 896.
12 F. W. McLafferty and F. Turecek, *Interpretation of Mass Spectra*, University Science Books, Mill Valley, CA, 4th edn, 1993.
13 S. P. Verevkin, B. Dogan, H. D. Beckhaus and C. Ruchardt, *Angew. Chem.*, 1990, **102**, 693.
14 Y. R. Luo, in *Handbook of Bond Dissociation Energy of Organic Compounds*, CRC Press, New York, 2003.
15 M. W. Chase, NIST-JANAF Thermodynamical Tables, *J. Phys. Chem. Ref. Data*, Monograph, 4th edn, 1998, vol. 9, ch. 4, p. 1.

16 W. Tsang, in *Energetics of Organic Free Radicals*, ed. J. A. Martinho Simoes, A. Greenberg and J. F. Liebman, Blackie Academic and Professional, London, 1996, p. 22.
17 (*a*) B. Li, N. Blough and P. Gutierrez, *Free Radical Biol. Med.*, 2000, **29**, 548; (*b*) X. Zhang, H. Wang and Y. Guo, *Rapid Commun. Mass Spectrom.*, 2006, **20**, 1877; (*c*) W. Adam, S. Bottle, R. Finzel, T. Kammel, E. Peters, K. Peters, H. Von Schnering and L. Walz, *J. Org. Chem.*, 1992, **57**, 982; (*d*) A. Beckwith and V. Bowry, *J. Org. Chem.*, 1989, **54**, 2681.
18 D. Duling, *J. Magn. Reson., Ser. B*, 1994, **104**, 105.



 